

Communication—In Situ Electrodeposition of Nickel Phosphide on Ni Foam for Non-Enzymatic Detection of Nitrite

To cite this article: Shun Lu *et al* 2020 *J. Electrochem. Soc.* **167** 146517

View the [article online](#) for updates and enhancements.



Communication—In Situ Electrodeposition of Nickel Phosphide on Ni Foam for Non-Enzymatic Detection of Nitrite

Shun Lu,^{1,*}  Matthew Hummel,^{1,*}  Xiaomei Wang,² Wei He,³ Rajesh Pathak,^{3,*} Xiuxiu Dong,⁴ Hongxing Jia,^{1,z} and Zhengrong Gu^{1,z}

¹Department of Agricultural and Biosystems Engineering, South Dakota State University, Brookings, South Dakota 57007, United States of America

²Research Center of Eco-environment and Resources, Chinese Academy of Fishery Sciences, Beijing 100141, People's Republic of China

³Department of Electrical Engineering and Computer Science, South Dakota State University, Brookings, South Dakota 57007, United States of America

⁴School of Agricultural Equipment Engineering, Jiangsu University, Zhenjiang, Jiangsu 212013, People's Republic of China

An electrochemical sensor toward nitrite based on Ni foam supported nickel phosphide (NiP/NF) electrode was successfully fabricated via an in situ electrodeposition strategy. The sensor has exhibited great electrochemical detection ability with a sensitivity of $1.56 \times 10^{-4} \text{ mA } \mu\text{M}^{-1}$, a linear range from 0.1 to 4000 μM and a detection limit of 0.01 μM ($s/n = 3$). Moreover, good stability of the electrodeposited electrode can be ascribed to the in situ growth of NiP onto Ni foam to achieve a binder-free electrode. The good recovery achieved for nitrite detection in several water samples also reveals its promising practicality.

© 2020 The Electrochemical Society ("ECS"). Published on behalf of ECS by IOP Publishing Limited. [DOI: [10.1149/1945-7111/abc99d](https://doi.org/10.1149/1945-7111/abc99d)]

Manuscript submitted July 15, 2020; revised manuscript received September 29, 2020. Published November 18, 2020.

Supplementary material for this article is available [online](#)

The detection of nitrite in drinking water and consumables is a critical process for preventing major threats to human health. While integral to normal body functions in low levels, large amounts of nitrite can lead to poisoning in the short-term and the development of cancers over an extended period of time,^{1,2} due to nitrite's interference with hemoglobin's oxygen transport role in the blood by irreversible binding.³ Current methods for detecting nitrite such as spectrophotometry and high-performance liquid chromatography are highly sensitive but cost-prohibitive and difficult to operate outside of the laboratory.⁴ Electroanalysis strategy is regarded as a promising approach to achieve excellent sensitivity and highly selectivity due to molecular redox on the surface of the working electrode. Electrode modification is of importance for improving sensitivity and anti-interference performance in this process.⁵⁻⁸ However, conventional electrode modifications were mainly based on glassy carbon electrode or screen-print electrode.^{6,9-12} It is difficult to achieve the modified electrode's maximum performance owing to the electrocatalyst is easily peeled off during electroanalysis. So, electrocatalyst grown on the electrode can efficiently solve this problem without any conductive binder through in situ synthesis.

Transition metal phosphides have drawn much attention in electrochemistry recently due to their excellent physicochemical properties, and facile synthesis process.¹³ Nickel phosphides (Ni_xP_y) have been successfully implemented as a low-cost, high performance material in hydrogen evolution reactions (HER) and oxygen evolution reactions (OER) due to the flexible valence state of phosphorous and their metalloid properties.¹³⁻¹⁵ NiP can also participate as an electrocatalyst in the oxidation of nitrite.^{12,16} Furthermore, Ni foam, which is a common, three-dimensional porous metallic material, offers many benefits as a substrate and electrode owing to its relatively low cost, high conductivity, and porosity. The porous structure of Ni foam provides more active sites and robust supports for efficient reactions at high current densities after modification.^{17,18} So, based on the mechanism of nitrite oxidation, NiP grown on Ni foam through the in situ electrodeposition for nitrite detection will maximize its exposure to nitrite and allow for a more sensitive system.

In this work, nickel phosphide was electrodeposited onto nickel foam as an electrochemical sensor and investigated for aqueous nitrite detection. Benefiting from the highly conductivity of Ni foam and excellent electrocatalytic performance of NiP, the working electrode presented a great detecting performance with the low limit of detection (0.01 μM , $s/n = 3$) and a sensitivity of $1.56 \times 10^{-4} \text{ mA } \mu\text{M}^{-1}$. The stability and anti-interference of the electrodeposited electrode were also investigated, respectively. The as-prepared electrochemical sensor was further applied for the determination of nitrite in real samples.

Experimental

Synthesis of NiP/Ni foam electrode.—The Ni foam (denoted as NF, area = $1.0 \times 2.0 \text{ cm}^2$, sheet thickness = 2 mm) was immersed in 1.0 M hydrochloric acid for 20 min and then in ethanol for 15 min under ultrasonic vibration to remove oxides and other substance, then it was washed with deionized water for several times. Briefly, the NF working electrode was immersed into a 50 mL 0.1 M acetate buffer solution ($\text{pH} = 7$) containing 0.05 M Nickel (II) acetate ($\text{Ni}(\text{CH}_3\text{COO})_2$) and 0.1 M sodium hypophosphite monohydrate (NaH_2PO_2). A saturated Ag/AgCl with KCl solution was used as the reference electrode, and a Pt wire was employed as the counter electrode. After 10-cycle CV scanning between -0.3 V and -1.0 V vs Ag/AgCl at a scan rate of 50 mV s^{-1} , NiP was uniformly electrodeposited on Ni foam, named as NiP/NF. The washed NF was used in this work for comparison.

Physical characterizations.—The phase structure of the NiP/NF was characterized by MiniFlex X-ray diffraction (XRD) using a RINT 2000 diffractometer (Rigaku Corporation, TX, USA) with $\text{Cu K}\alpha$ radiation ($\text{Cu-K}\alpha$ radiation wavelength of $\lambda = 1.5406 \text{ \AA}$). The XRD patterns were analyzed with MDI-jade V5.0 software (Rigaku Corporation). The morphology of the electrodeposited NiP/NF was observed using the field emission scanning electron microscopy (Hitachi S-4300N). Energy-dispersive X-ray (EDX, INCA) spectra were recorded (resolution at 5.9 keV).

Electrochemical measurements.—The electrochemical measurements were carried out using CHI-760E (Texas, USA) workstation. A conventional three-electrode setting with NF as a working electrode (2 cm^2), Ag/AgCl as a reference electrode (electrolyte: saturated KCl), and Pt wire as the counter electrode was used. 0.1 M

*Electrochemical Society Student Member.

^zE-mail: matthew.j.hummel@sdstate.edu; hongxing.jia@sdstate.edu; zhengrong.gu@sdstate.edu

phosphate buffers solution (PBS, pH 7.0) was used in the whole electrochemical tests. Amperometric measurements were performed. Electrochemical impedance spectroscopy (EIS) measurements were performed (parameters setting: 10 mV amplitude AC signal, frequency ranging from 100 kHz to 1 Hz) and EIS results were simulated by Zview software (v. 3.5 h). All potentials employed in this study were vs Ag/AgCl unless otherwise stated. Compensation for iR drop was used for all cyclic voltammograms (CVs).

Results and Discussion

As presented in Scheme 1, NiP/NF was prepared by an in situ electrodeposition route that nickel phosphide was formed from electrolytes containing $\text{Ni}(\text{CH}_3\text{COO})_2$ and NaH_2PO_2 under consequent CVs scanning (10-cycle, -0.2 to -1.0 V vs Ag/AgCl) (Fig. S1 is available online at stacks.iop.org/JES/167/146517/mmedia). The electrodeposited electrode was rinsed and dried in the air after electrodeposition, then it would be subjected to the next characterizations, i.e. SEM, EDX, and XRD. Ni foam was also employed in this study as control studies to evaluate the difference in morphology, structure, and electrochemical performance.

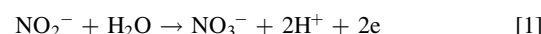
The surface morphology of NiP/NF electrode was observed by SEM, as shown in Fig. 1a. A typically porous network-like porous structure was clearly observed for Ni foam, which provided sufficient internal surface area for material adsorption. After electrodeposition, NiP was uniformly grown on the surface of Ni foam through SEM observation. The homogeneous dispersion of Ni and P was confirmed by the EDX-mapping analysis (inset of Figs. 1a and S2). Meanwhile, two elements of Ni and P were also detected by EDX spectrum, as shown in Fig. S2. However, it is difficult to confirm whether Ni element came from NiP/NF or Ni foam only in terms of EDX results. So, XRD analysis is used to further confirmation. Figure 1b depicts the XRD patterns of NiP/NF and Ni foam. It is easily found that two strong peaks located in $45.25^\circ/52.56^\circ$ for Ni foam, and $44.97^\circ/52.28^\circ$ for NiP/NF, respectively. But there is a slightly left shift for NiP/NF compared with Ni foam. Similarly, Song et al. prepared bimetallic phosphides ($\text{Co}_x\text{Ni}_y\text{P}@\text{NF}$) for hydrogen production,¹⁹ and there is a similar phenomenon that diffraction peak of $\text{Co}_x\text{Ni}_y\text{P}@\text{NF}$ around 41° was shifted to the right with the increasing ratio of cobalt and nickel. The phenomenon in this study also indicates that the introduction of new species on the Ni foam will change the original crystalline structure of Ni foam after electrodeposition, further confirmed that NiP was successfully electrodeposited on the Ni foam combining previous SEM and EDX results.

CV, EIS, and amperometric $i-t$ response were employed in this study for nitrite detection. CV was used to evaluate the electrocatalytic performance of NiP/NF and Ni foam electrodes. As displayed in Fig. 2a, Ni foam electrode shows the same current response in the presence of nitrite or not. However, there is a catalytic oxidation peak at ~ 0.85 V (Fig. 2a) as nitrite added for NiP/NF electrode and NiP/NF electrode shows larger electrochemical surface than that of Ni foam in term of the closed CV areas,

indicating that (i) the introduction of NiP on Ni foam could increase more active sites for nitrite oxidation, (ii) NiP/NF electrode could promote fast electron transfer for nitrite oxidation. To further confirm the above points, CVs of NiP/NF and Ni foam electrodes in 0.1 M $\text{K}_3\text{Fe}(\text{CN})_6$ with saturated KCl solution were performed (Fig. S3). It can be seen that reversible redox peaks were obtained at Ni foam electrode; however, NiP/NF electrode presented a significant increase both in anodic and cathodic currents under the same conditions. The double-layer capacitance (C_{dl}) was also used to evaluate the electrochemical surface area of NiP/NF and Ni foam electrodes here (Fig. S4), which was performed by CV with a series of scan rates in a narrow potential range (nonfaradaic area, from -0.2 to -0.3 V). As a result, the C_{dl} of NiP/NF is larger than that of Ni foam (Fig. S4c). Not limited to the electrochemical surface area, active sites can promote the electrochemical oxidation of nitrite, the conductivity of the working electrode also plays an important role in electrochemical sensing.^{20,21} Therefore, EIS was employed here to study the conductivity of working electrodes (Fig. S4d). After modeling and simulation (Figs. S5–S6, Table S1), the charge transfer resistance (R_{ct}) of the working electrodes is calculated by the diameter of the semicircle in the Nyquist plots. The R_{ct} value of NiP/NF and Ni foam electrode are 30.79 and $31.27\ \Omega$, respectively. To some extent, the electrodeposited electrode performed better conductivity due to the parallel circuit between NiP and Ni foam.

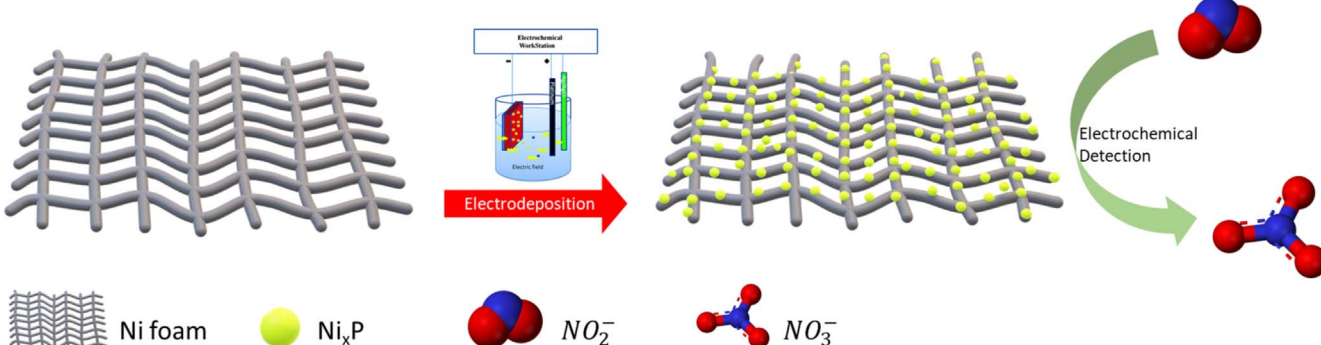
Accordingly, the advantages of NiP/NF employed in this study were fully presented.

Generally, two electrons of nitrite were transferred in this electrochemical oxidation as shown in Eq. 1:^{6,22}



To gain acquaintance with the mechanism of the nitrite oxidation taking place at NiP/NF electrode, the amperometric $i-t$ response was performed. Figure S7 depicts the amperometric $i-t$ response of NiP/NF electrode in 1.0 mM of nitrite. The relationship between current and against minus square root of time tends to a straight line with the calibration equation of $I/\text{mA} = 0.1x + 0.099$ ($R^2 = 0.995$), as presented in Fig. 2b. It is verified that the oxidation of nitrite on the NiP/NF electrode is a typical diffusion-controlled process.⁶ Therefore, amperometry was suited to the electrochemical detection of nitrite in the next electrochemical measurements.

Encouraged by the above results, electrochemical detection of nitrite under mild conditions was investigated over the NiP/NF electrode. Prior to using NiP/NF to detect nitrite, the applied potential needs to be optimized due to different potentials that have a non-negligible impact on electroanalysis.⁶ Then, the optimized potential (0.8 V vs Ag/AgCl) was selected for the electrochemical determination of nitrite in this work (Fig. S8). The amperometric response of NiP/NF electrode with the successive addition of nitrite under an optimized potential of 0.8 V under stirring was studied and the result is shown in Fig. 3a. When a certain amount of nitrite was added to the PBS solution, the fast attainment of a steady-state condition was observed. The calibration



Scheme 1. Illustration of preparation of NiP/Ni foam via electrodeposition method.

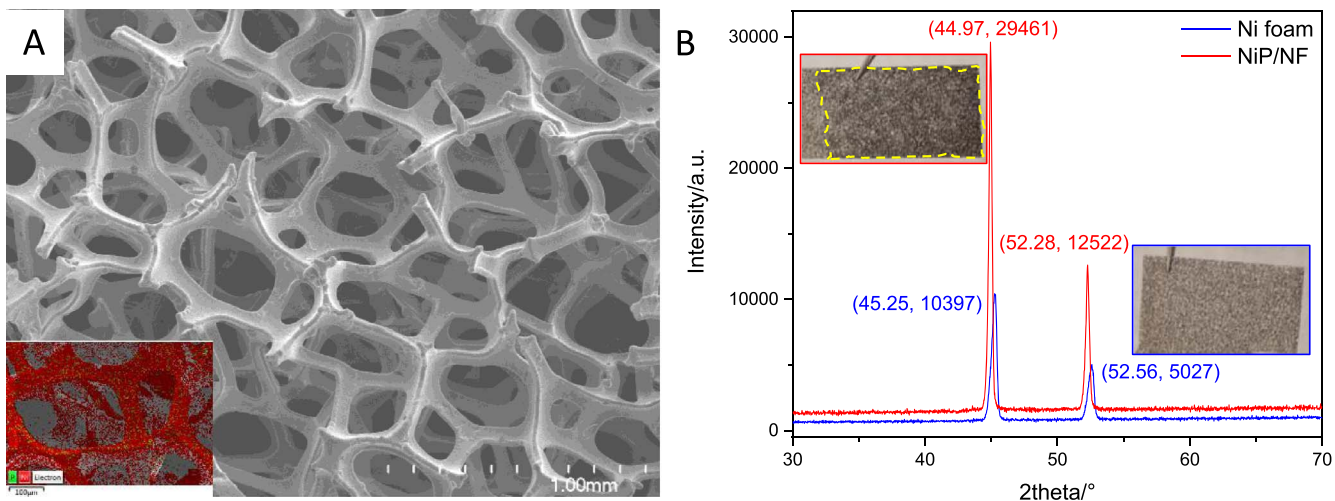


Figure 1. (a) SEM image of NiP/NF, inset: EDX mapping of NiP/NF; (b) XRD patterns of Ni foam (blue line) and NiP/NF (red line).

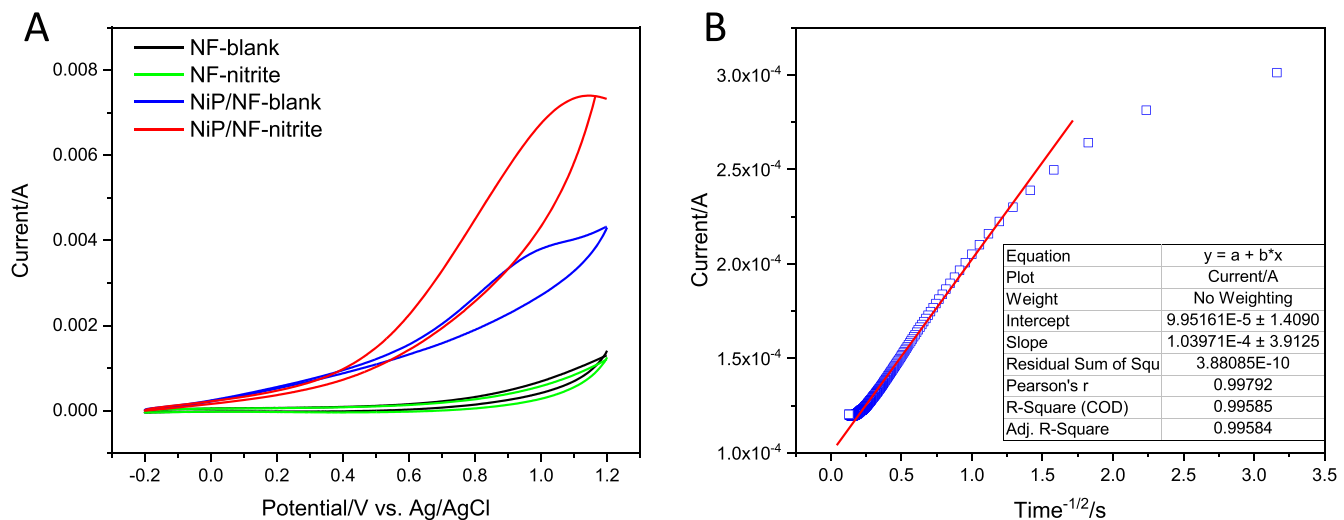


Figure 2. (a) CV curves of NiP/NF and Ni foam in absence and presence of nitrite in 0.1 M PBS; (b) The relationship of current and the time ($t^{-1/2}$) which derived from the amperometric i - t response (Fig. S7, test conditions: 0.1 M PBS (pH 7.0) containing 1.0 mM of nitrite under an applied potential of 0.8 V).

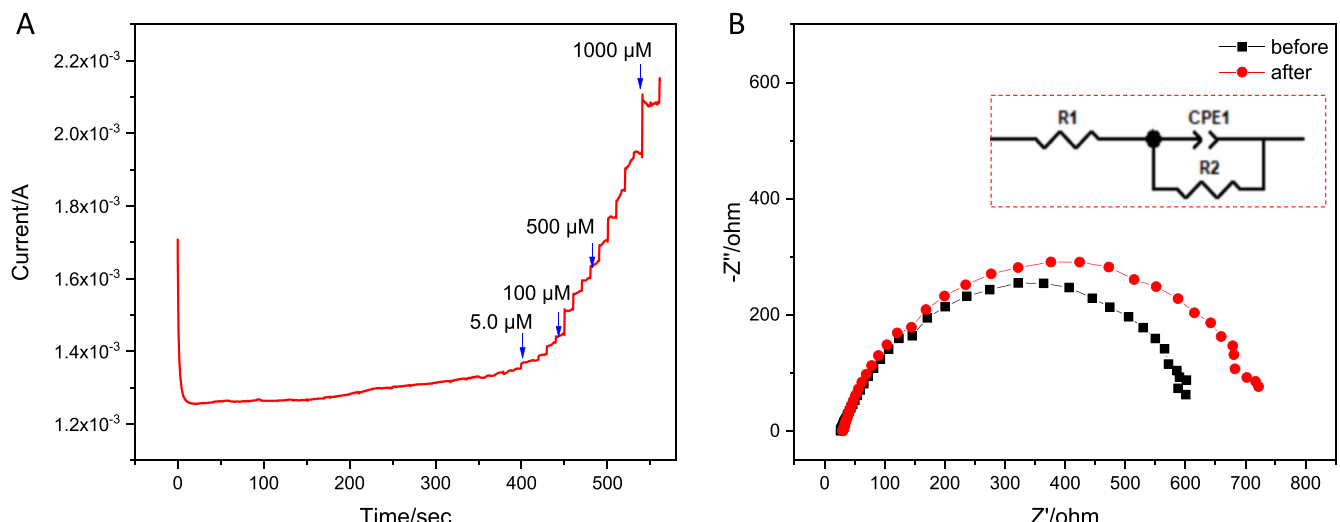


Figure 3. (a) Amperometric responses of nitrite on NiP/NF upon successive addition of nitrite to 0.1 M PBS (pH 7.0) under an applied potential of 0.8 V; (b) The comparison of Nyquist plots of NiP/NF between before and after nitrite detection.

curve for the nitrite detection obtained from the amperometric curve is shown in Fig. S9. The electrodeposited electrode showed a good linear relationship between current and nitrite concentration with calibration curves ($I/A = 0.540x/A \mu M^{-1} + 0.0014$, $x \in 0.1\text{--}500 \mu M$) and $I/A = 0.156 y/A \mu M^{-1} + 0.00154$, $y \in 500\text{--}4000.0 \mu M$) with a correlation coefficient of 0.989 and 0.999, respectively. The limit of detection (LOD) were calculated as $0.02 \mu M$ and $0.01 \mu M$ ($s/n = 3$). To further access the detective performance of the electrodeposited electrode over nitrite sensing, the comparison of our study with other recent reports was conducted, as listed in Table SII. Apparently, the NiP/NF electrode presented a decent performance towards electrochemically nitrite detection.

In addition, the NiP/NF electrode also needs excellent selectivity toward common interfering before the practical application. To evaluate the selectivity of NiP/NF electrode toward nitrite detection, the influence of interfering species was tested by amperometry test with the same set of Fig. 3a. Different substances, such as $NaNO_3$, CH_3COONa , KCl , Cu_2SO_4 , dopamine, and glucose at a concentration of 100-fold as much as of nitrite ($5.0 \mu M$), were used for the interfering test. As presented in Fig. S10, the current increases immediately upon the introduction of nitrite, whereas the successive addition of interferes did not produce any significantly current alteration. In addition, further injection of $5.0 \mu M$ nitrite results in the same stair-like current response as the previous nitrite addition. The results indicate that the presence of these coexisting species does not influence nitrite detection. The stability is another important index of the electrochemical sensor for practical applications. As can be seen from Fig. 3b, the R_{ct} value of NiP/NF (27.38Ω , Fig. S11) after nitrite detection is almost no change compared to before electrochemical measurements (30.79Ω). Moreover, its current signal is also kept relatively stable after 10 h $i-t$ test (Fig. S12). These results concluded that the electrodeposited NiP/NF electrode possessed good electrochemical selectivity and stability toward nitrite detection.

To evaluate the reliability and efficiency of the NiP/NF for practical application, the relative standard deviation (RSD) for three individual NiP/NF was calculated by sensing a series concentration of nitrite ($0.5 \mu M$, $200 \mu M$ and $1000 \mu M$) with the same method in the 0.1 M PBS and drinking water. All the water samples were received pretreatment before detection. As shown in Table SIII ($n = 3$), all results from drinking water are in good agreement with standard samples' results in 0.1 M PBS. The RSD of the current response was low than 4.5% with good recovery, indicating that the electrodeposited electrode has good reproducibility.

Conclusions

In summary, an electrochemical sensor toward nitrite based on Ni foam-supported nickel phosphide electrode was successfully fabricated via an *in situ* electrodeposition strategy. The sensor has exhibited great electrochemical detection ability with a sensitivity of $1.56 \times 10^{-4} \text{ mA } \mu M^{-1}$, a linear range from 0.1 to $4000 \mu M$ and a detection limit of $0.01 \mu M$ ($s/n = 3$). These good performances can be attributed to the simple *in situ* electrodeposition and great electrocatalytic performance of NiP. Moreover, good stability of the electrodeposited electrode can be ascribed to the *in situ* growth route to construct a binder-free electrode. These results provide a new way to fabricate a novel electrochemical nitrite sensor. Further works will be carried out to investigate the properties of M-P, (M refers to Fe, Co, Mn, Cu, etc.) to detect nitrite.

Acknowledgments

This work was supported by NSF EPSCoR (No. OIA-1849206), NASA EpsCor (No. NNX16AQ98A) and USDA-NIFA Hatch (No. SD00H618-16, SD00R680-19 NC1194). S. Lu also thanks Prof.

Parashu Kharel's assistance for XRD measurements. The authors want to thank South Dakota 2D Materials for Biofilm Engineering, Science and Technology Center (2DBEST) for supporting this project.

ORCID

Shun Lu  <https://orcid.org/0000-0003-4287-0779>
Matthew Hummel  <https://orcid.org/0000-0002-9576-1309>

References

1. J. Sanchez-Echaniz, J. Benito-Fernández, and S. Mintegui-Raso, "Methemoglobinemia and consumption of vegetables in infants." *Pediatrics*, **107**, 1024 (2001).
2. Z. Dai, H. Bai, M. Hong, Y. Zhu, J. Bao, and J. Shen, "A novel nitrite biosensor based on the direct electron transfer of hemoglobin immobilized on CdS hollow nanospheres." *Biosens. Bioelectron.*, **23**, 1869 (2008).
3. M. Parvizishad, A. Dalvand, A. H. Mahvi, and F. Goodarzi, "A review of adverse effects and benefits of nitrate and nitrite in drinking water and food on human health." *Health Scope*, **6**, e14164 (2017).
4. Q.-H. Wang, L.-J. Yu, Y. Liu, L. Lin, R.-G. Lu, J.-P. Zhu, L. He, and Z.-L. Lu, "Methods for the detection and determination of nitrite and nitrate: a review." *Talanta*, **165**, 709 (2017).
5. Z. Yilong, Z. Dean, and L. Daoliang, "Electrochemical and other methods for detection and determination of dissolved nitrite: a review." *Int. J. Electrochem. Sci.*, **10**, 1144 (2015).
6. S. Lu, M. Hummel, S. Kang, and Z. Gu, "Selective voltammetric determination of nitrite using cobalt phthalocyanine modified on multiwalled carbon nanotubes." *J. Electrochem. Soc.*, **167**, 046515 (2020).
7. S. Lu, M. Hummel, K. Chen, Y. Zhou, S. Kang, and Z. Gu, "Synthesis of Au@ZIF-8 nanocomposites for enhanced electrochemical detection of dopamine." *Electrochim. Commun.*, **114**, 106715 (2020).
8. S. Lu, Z. Gu, M. Hummel, Y. Zhou, K. Wang, B. B. Xu, Y. Wang, Y. Li, X. Qi, and X. Liu, "Nickel oxide immobilized on the carbonized eggshell membrane for electrochemical detection of urea." *J. Electrochem. Soc.*, **167**, 106509 (2020).
9. Z. Zhao, J. Zhang, W. Wang, Y. Sun, P. Li, J. Hu, L. Chen, and W. Gong, "Synthesis and electrochemical properties of Co3O4-rGO/CNTs composites towards highly sensitive nitrite detection." *Appl. Surf. Sci.*, **485**, 274 (2019).
10. L. Li, D. Liu, K. Wang, H. Mao, and T. You, "Quantitative detection of nitrite with N-doped graphene quantum dots decorated N-doped carbon nanofibers composite-based electrochemical sensor." *Sensors Actuators B*, **252**, 17 (2017).
11. M. Saraf, R. Rajak, and S. M. Mobin, "A fascinating multitasking Cu-MOF/rGO hybrid for high performance supercapacitors and highly sensitive and selective electrochemical nitrite sensors." *Journal of Materials Chemistry A*, **4**, 16432 (2016).
12. S. Lu, C. Yang, and M. Nie, "Hydrothermal synthesized urchin-like nickel-cobalt carbonate hollow spheres for sensitive amperometric detection of nitrite." *J. Alloys Compd.*, **708**, 780 (2017).
13. S. Anantharaj, S. R. Ede, K. Sakthikumar, K. Karthick, S. Mishra, and S. Kundu, "Recent trends and perspectives in electrochemical water splitting with an emphasis on sulfide, selenide, and phosphide catalysts of Fe, Co, and Ni: a review." *ACS Catal.*, **6**, 8069 (2016).
14. X. Yu, Z.-Y. Yu, X.-L. Zhang, Y.-R. Zheng, Y. Duan, Q. Gao, R. Wu, B. Sun, M.-R. Gao, and G. Wang, "'Superaerophobic' nickel phosphide nanoarray catalyst for efficient hydrogen evolution at ultrahigh current densities." *JACS*, **141**, 7537 (2019).
15. Z. Li, X. Dou, Y. Zhao, and C. Wu, "Enhanced oxygen evolution reaction of metallic nickel phosphide nanosheets by surface modification." *Inorganic Chemistry Frontiers*, **3**, 1021 (2016).
16. Z. Fu-ling, X. Xiao-li, and S. Xu-ping, "High-efficiency nitrite sensor based on CoP nanowire array." *Journal of Electrochemistry*, **25**, 252 (2019).
17. X. Shang, J.-Q. Chi, S.-S. Lu, B. Dong, Z.-Z. Liu, K.-L. Yan, W.-K. Gao, Y.-M. Chai, and C.-G. Liu, "Hierarchically three-level Ni3 (VO4) 2@ NiCo2O4 nanostructure based on nickel foam towards highly efficient alkaline hydrogen evolution." *Electrochim. Acta*, **256**, 100 (2017).
18. X. Lu and C. Zhao, "Electrodeposition of hierarchically structured three-dimensional nickel-iron electrodes for efficient oxygen evolution at high current densities." *Nat. Commun.*, **6**, 1 (2015).
19. Y. Du, G. Pan, L. Wang, and Y. Song, "CoxNiyp embedded in nitrogen-doped porous carbon on Ni foam for efficient hydrogen evolution." *Appl. Surf. Sci.*, **469**, 61 (2019).
20. S. Lu, M. Hummel, Z. Gu, Y. Gu, Z. Cen, L. Wei, Y. Zhou, C. Zhang, and C. Yang, "Trash to treasure: a novel chemical route to synthesis of NiO/C for hydrogen production." *Int. J. Hydrogen Energy*, **44**, 16144 (2019).
21. M. Nie, X. Liu, B. He, Q. Li, S. Du, S. Lu, C. Jiang, and D. Lei, "Investigation of the AuPdPt-WC/C electrocatalyst for hydrogen evolution reaction." *J. Electrochem. Soc.*, **163**, H485 (2016).
22. R. Guidelli, F. Pergola, and G. Raspi, "Voltammetric behavior of nitrite ion on platinum in neutral and weakly acidic media." *Anal. Chem.*, **44**, 745 (1972).